

State selected removal of vibrationally excited $\text{NH}_2[X^2B_1(0, \nu_2, 0)]$ radicals

Karl-Heinz Gericke, Lourdes M. Torres, and William A. Guillory
Department of Chemistry, University of Utah, Salt Lake City, Utah 84112

(Received 4 January 1984; accepted 13 March 1984)

The influence of vibrational excitation on the decay rate of NH_2 radicals in the presence of selected substrates has been studied using the laser-induced fluorescence (LIF) technique. The NH_2 radicals were generated by infrared multiple photon dissociation (IRMPD) of selected precursors (N_2H_4 , CH_3NH_2), and the state selected $\text{NH}_2(\nu_2'' = 0, 1)$ decay was observed by means of the sensitive LIF measurement of $[\text{NH}_2]$. The reactions studied were of the type: $\text{NH}_2(\nu_2'' = 0, 1) + \text{R} \rightarrow \text{products}$, with $\text{R} = \text{NO}$, CH_3NH_2 , N_2H_4 . The reaction rates were determined under pseudo-first-order conditions, and were found to be strongly dependent on the vibrational state of the NH_2 radical, e.g., $k_{\text{NO}}(\nu_2'' = 0) = 1.4 \times 10^{-11} \text{ cm}^3 \text{ molecule}^{-1} \text{ s}^{-1}$ and $k_{\text{NO}}(\nu_2'' = 1) = 3.2 \times 10^{-11} \text{ cm}^3 \text{ molecule}^{-1} \text{ s}^{-1}$. This influence of vibrational excitation on the total decay rates is discussed and compared with previously reported data on thermal excitation. In thermal studies of these same chemical reactions, a negative temperature coefficient was found for the reaction rate constants. The contribution of diffusion and of vibrational relaxation processes is also considered, as well as the relative importance of the two-body vs the three-body collision reaction channels: $\text{NH}_2 + \text{NH}_2 \rightarrow \text{NH}_3 + \text{NH}$ and $\text{NH}_2 + \text{NH}_2 + \text{M} \rightarrow \text{N}_2\text{H}_4 + \text{M}$ for $\text{M} = \text{O}_2$, N_2 , and Ar .

INTRODUCTION

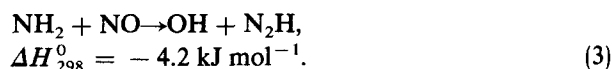
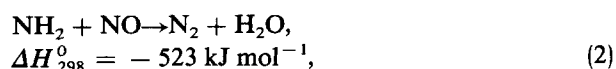
The energy dependence of a chemical reaction is usually studied under conditions in which collisional energy transfer is fast compared to the reaction rate, i.e., the energy content of the reactants is determined by its temperature. However, the temperature dependence of the reaction rate contains no specific information on how any other particular distribution of the energy through the different degrees of freedom affects the reaction rate; that is, how specific excitation of translation, vibration, or rotation of the reacting molecules, contributes to overcoming the potential energy barrier. If the influence of the excited states of various degrees of freedom on the reaction path is known, then the chemical reaction can be driven more selectively than by simple thermal heating. Such information can also be used to understand, in more detail, the reaction contribution made by rotationally and vibrationally excited species, in combustion and flame processes.

The vibrationally excited species to be discussed in this paper is $\text{NH}_2(0, \nu_2, 0)$, in the reaction



This reaction has been found to be of great importance in combustion and atmospheric processes,¹⁻³ and consequently several studies have been made in order to determine the major products, reaction channels, and temperature dependence of the reaction rates⁴⁻⁸ of this system.

The possible reaction channels have been studied by several groups.⁴⁻⁸ Gehring and his co-workers⁴ found the main reaction products (95%) to be N_2 and H_2O . More recently, using the laser-induced fluorescence technique, Silver and Kolb⁵ detected the presence of a minor amount (~5%) of OH , but no H radicals. Based on these data, the two main channels appear to be:

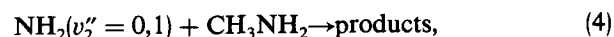


The temperature dependence studies made on this system by Hack *et al.*⁷ and Lesclaux *et al.*⁸ showed a negative temperature coefficient for the reaction rate in the region between 210 and 500 K. Similar results were reported by Silver and Kolb⁵ for the wider range 294–1500 K, confirming that a decrease in the reaction rate is brought about by an increase in the system temperature.

In light of these observations, it is of interest to study the dependence of the removal rate of state selected NH_2 radicals which have a nonequilibrium population of excited states. Translational and rotational relaxation of the reactants is expected to occur in a few gas kinetic collisions, but longer lifetimes are expected of excited vibrational states due to the larger energy spacing between the vibrational levels.

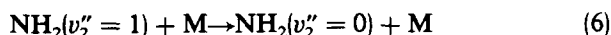
It has been demonstrated that infrared multiple photon dissociation (IRMPD) of selected precursor molecules is an excellent source of radicals having a nonequilibrium energy distribution among the different degrees of freedom.⁹⁻¹² The sensitive laser-induced fluorescence (LIF) method is used to probe state selected radicals in order to obtain reaction rates for reaction (1) with NH_2 in either the $\nu_2'' = 0$ or $\nu_2'' = 1$ state with $\text{NO}(\nu'' = 0)$. For simplicity, the $\text{NH}_2[X^2B_1(0, 1, 0)]$ state is referred to hereafter as $\text{NH}_2(\nu_2'' = 1)$ and $\text{NH}_2[X^2B_1(0, 0, 0)]$ as $\text{NH}_2(\nu_2'' = 0)$.

It is also necessary to consider the effect of vibrational relaxation on the observed decay rates of $\text{NH}_2(\nu_2'' = 1)$, as well as the influence of $\text{NH}_2(\nu_2'' = 0, 1)$ reactions with the precursor molecules



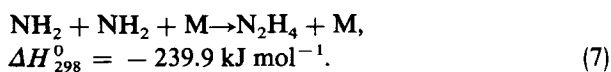
As a result, the rate constants of processes (1), (4), (5),

and

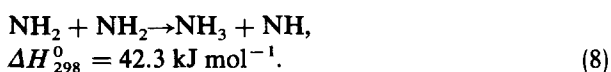


were determined.

In addition, the reaction paths of selected radical-radical reactions were investigated. The combination of NH_2 radicals according to reaction (7) below, has been found to be the mechanism responsible for the formation of hydrazine in various systems in which photolysis radiolysis, and discharges of suitable precursors have been used to study NH_2 radicals,¹³



The hydrazine yield in these systems obviously depends on the reaction rate, but no reliable data are known for this reaction as is discussed in the work of Baulch *et al.*¹³ One of the principal reasons for this lack of definitive information is the fact that, in the past, reaction (8) below has been consistently overlooked by a number of authors who tried to interpret the NH_2 decay solely in terms of reaction (7),



Salzman and Bair¹⁴ have demonstrated that both reactions are competitive. Later, Gehring *et al.*⁴ obtained for the first time a value for k_8/k_7 :

$$k_8/k_7 = 1.3 \times 10^{17} \text{ molecules cm}^{-3},$$

which shows the much greater importance of reaction (8) over reaction (7) at pressures less than ~ 1 Torr.

The IRMPD of N_2H_4 produces a relatively high concentration of amino radicals, so that it was possible to determine the rate of removal of NH_2 by each radical-radical reaction channel above. By varying the pressure of the third body collision partner M, one can distinguish between the two reaction channels. Consequently, the ratio of k_8/k_7 could also be determined.

In order to study the influence of third body-type collision partners in the stabilization of the NH_2 - NH_2 complex, N_2 and O_2 , and Ar were selected as molecular and atomic collision partners, respectively.

EXPERIMENTAL

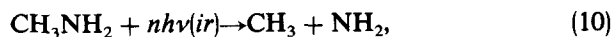
The experiments were performed using a Gen-Tec DD250 CO_2 laser as a high intensity IR source, and a Molecron UV/400/DL 200 N_2 pumped dye laser as a probe source. The NH_2 radicals were generated by IRMPD of hydrazine, N_2H_4 , and monomethylamine, CH_3NH_2 , as precursors. Hydrazine is the more efficient precursor in terms of the total number of NH_2 radicals formed,¹⁶ occurring through a simple two-center N-N bond breaking which leads to the production of two amino radicals,



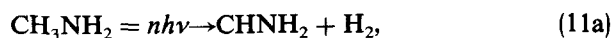
The NH_2 radicals from this reaction are primarily formed in the $\nu_2'' = 0$ state.

Although the total number of amino radicals formed by IRMPD of monomethylamine is smaller than in the case of N_2H_4 , a substantially greater fraction of radicals are formed

in vibrationally excited states.^{16,17} The two most likely fragmentation processes for monomethylamine bond breaking are¹⁶ the two-center C-N bond breaking,



and the two step process¹⁷



The NH_2 radicals were generated in a fluorescence chamber made of stainless steel. Three sets of entrance and exit windows were set at right angles to each other: one for the CO_2 laser beam with which the radicals were generated, one for the dye laser beam with which the NH_2 radicals were probed, and one for the total fluorescence light.

The lasers were operated at a 20 pps repetition rate. The CO_2 laser beam had an output energy of 0.5 J/pulse with a temporal shape of a 200 ns wide initial spike, followed by a 3 μs tail. To obtain good time-resolved measurements which are not influenced by the width of the CO_2 laser even at higher pressures, most experiments were performed by eliminating N_2 from the CO_2 laser gas mixture. This results in a decrease of the output energy (down to 100 mJ), but it also reduces the temporal width of the beam to solely a 200 ns wide spike. The CO_2 laser beam was tuned to the $P(20)$ line of the $00^{\circ}1 - 02^{\circ}0$ transition at 9.552 μm and focused by a 15 cm focal length ZnSe lens through a NaCl window into the cell. The emitted wavelength falls within the band center of the ν_8 "C-N stretching" vibration of CH_3NH_2 (overlapping the R branch)¹⁸ and it also overlaps the ν_4 symmetric rocking vibration of the N_2H_4 PQ branch.¹⁹

A 1×10^{-2} M dye solution of 7D4TMC in *p*-dioxane was used in the dye laser to monitor the ground state NH_2 radicals. An optimum detection of $\text{NH}_2(X^2B_1)$ was achieved when the $^PQ_{1,3}$ transition of the $\text{NH}_2[A^2A_1(0,13,0) \leftarrow X^2B_1(0,0,0)]$ band was pumped.^{20,21} The dye laser beam (2 mm diameter) had an output energy of 70 μJ and passed through a series of baffles to reduce the scattered light before it reached the reaction zone. For the studies made on vibrationally excited states, a 1×10^{-2} M solution of Coumarin 485 in ethanol was used to excite the $^PQ_{1,3}$ transition of the $\text{NH}_2[A^2A_1(0,13,0) \leftarrow X^2B_1(0,1,0)]$ band. A low resolution monochromator, a Jobin-Yvon 0.1 m (2 mm slit width), followed by an EMI 9635B photomultiplier tube (bialkali response) collected the LIF at right angles with respect to the two laser beams. The monochromator was set at 533 nm [$A^2A_1(0,13,0) \rightarrow X^2B_1(0,1,0)$] to observe the fluorescence for the $\text{NH}_2(\nu_2'' = 0)$ measurements, and at 492 nm [$A^2A_1(0,13,0) \rightarrow X^2B_1(0,0,0)$] for the $\text{NH}_2(\nu_2'' = 1)$ experiments. With this experimental arrangement, the scattered light was less than one photon per laser shot.

The electrical signal was then integrated over the total fluorescence time using a gated integrator (Boxcar PAR 162/164), digitized, and collected by a Nicolet 1070 multi-channel averager. The data were then transferred to a Terak 8500 minicomputer for further analysis, and finally plotted on a Tektronix 4662 plotter.

The CO_2 and the N_2 pumped dye lasers were synchronously triggered utilizing an external reference trigger. The

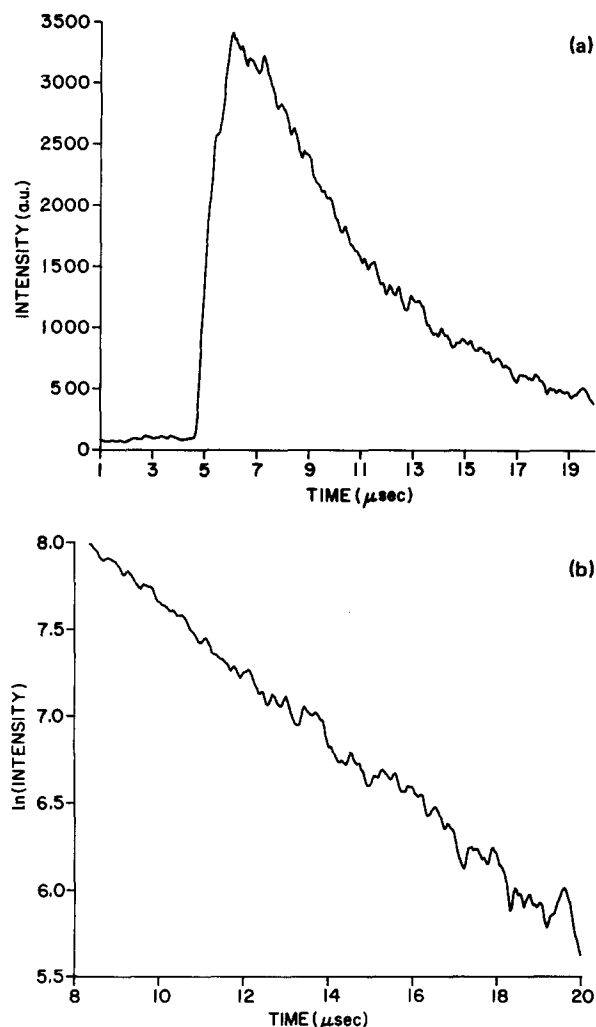


FIG. 1. Decay curve for $\text{NH}_2(v'' = 1) + \text{NO}$. (a) Laser-induced fluorescence signal $\text{Int}(t)$ from $\text{NH}_2(v'' = 1)$, as a function of time for a mixture of 50 mTorr CH_3NH_2 , 52 mTorr NO , 2 Torr Ar. The curve is 512 points wide, and each point is an average of ten laser shots. (b) Logarithm of the signal intensity as a function of time for a mixture of 50 mTorr CH_3NH_2 , 52 mTorr NO , and 2 Torr Ar, showing the pseudo-first-order behavior. The rate constant can be obtained from the negative slope of the curve.

variable delay between the two lasers was scanned through the time domain of the experiment with the aid of a modified Evans Assoc. Model 4141 Programmable Time Delay Module. The time resolution of these experiments was controlled by the experimental time domain set by the scan delay generator and the number of memory locations of the multichannel analyzer used to collect the data. Each scan of the probe laser delay time with respect to the CO_2 pump laser consisted of 512 points. For weak signals, the delay sweep was repetitively scanned.

Time decay plots, as shown, for example, in Fig. 1(a), were obtained for different pressures of N_2H_4 , CH_3NH_2 , NO , Ar, N_2 , and O_2 . The pressures were recorded with a Diametrics 570A capacitance manometer, and different ranges were used for the determination of the decay rates: Precursor pressures ranged from 5–50 mTorr; O_2 and N_2 pressures from 1–115 Torr; Ar pressures from 0.5–130 Torr; and NO pressures from 50 mTorr–3 Torr.

It is important to mention that the various reactants do

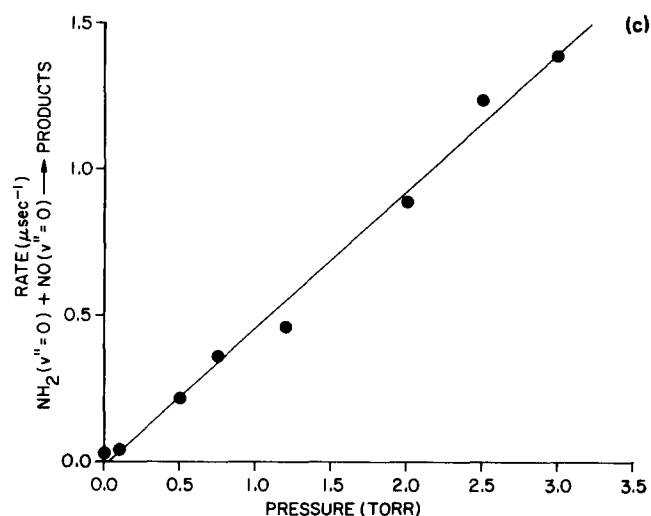


FIG. 2. Pseudo-first-order rate constant values for the $\text{NH}_2(v'' = 0) + \text{NO}(v'' = 0)$ reaction as a function of NO pressure. From the slope, the second-order rate constant is obtained. CH_3NH_2 precursor pressure 50 mTorr and 2 Torr Ar.

influence the radiative lifetimes of $\text{NH}_2(A^2A_1)$. The rate constants, however, are measured under pseudo-first-order conditions $[\text{R}] \gg [\text{NH}_2]$, i.e., the reactant concentration is much greater than the amino radical concentration. Consequently, the quenching effects due to reactant species do not change with reaction time.

The decay rates were determined from semilog plots of the observed time scans. One example of a representative semilog plot is shown in Fig. 1(b).

RESULTS AND DISCUSSION

State selected removal of $\text{NH}_2(v''_2 = 0)$ with $\text{NO}(v'' = 0)$

The rates of reaction and of the relaxation processes of NH_2 were obtained by time-resolved experiments in which the removal of $\text{NH}_2(v''_2 = 0, 1)$ was detected by using the sensitive LIF technique. Pseudo-first-order kinetics were assumed since, at all points, the reactant pressure was much greater than the maximum possible NH_2 concentration.

In order to sufficiently reduce the diffusion of NH_2 out of the probe zone such that diffusion is slow as compared to

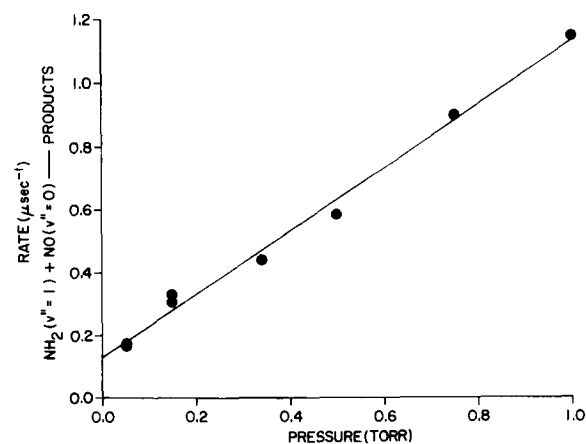


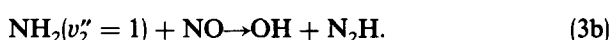
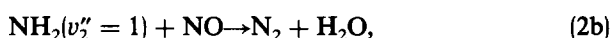
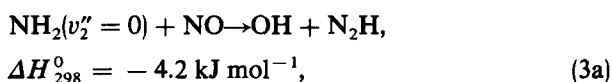
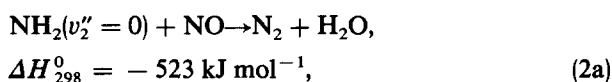
FIG. 3. Same as Fig. 2, but for the reaction $\text{NH}_2(v'' = 1) + \text{NO}(v'' = 0)$. CH_3NH_2 precursor pressure 50 mTorr and 2 Torr Ar.

TABLE I. Experimental rate determinations for NH_2 and selected literature values.

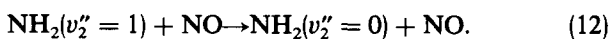
Reaction	Rate constant ($T = 298 \text{ K}$) ($\text{cm}^3 \text{ molecule}^{-1} \text{ s}^{-1}$)	Method	Reference
$\text{NH}_2(\nu_2'' = 0) + \text{NO}(\nu'' = 0)$	$(0.96 \pm 0.24) \times 10^{-11}$	Flow reactor	5
	$(2.1 \pm 0.2) \times 10^{-11}$	Flash photolysis	6
	$(1.4 \pm 0.1) \times 10^{-11}$	MPD/LIF	This work
	1.2×10^{-11}	Flow reactor	7
	$(1.7 \pm 0.4) \times 10^{-11}$	Flash photolysis	8
$\text{NH}_2(\nu_2'' = 1) + \text{NO}(\nu'' = 0)$	$(3.2 \pm 0.2) \times 10^{-11}$	MPD/LIF	This work
$\text{NH}_2(\nu_2'' = 1) + \text{CH}_3\text{NH}_2$	$(7.7 \pm 0.9) \times 10^{-11}$	MPD/LIF	This work
$\text{NH}_2(\nu_2'' = 1) + \text{N}_2\text{H}_4$	$(9.0 \pm 1.5) \times 10^{-11}$	MPD/LIF	This work

the other removal rates of NH_2 , variable pressures of added Ar were used (~ 2 Torr). In the very dense time sampling (512 points per time scan) of the decay curve, the influence of diffusion can be easily observed, because the signal decay in such cases follows a different time behavior than the reactions or relaxation of NH_2 .^{10,22} The negative slope of a graph of $\ln(\text{Int})$ vs time, where Int is the NH_2 fluorescence signal intensity, is then the pseudo-first-order rate constant. Figure 2 shows the variation of the observed decay rates of NH_2 in the vibrational ground state vs NO pressures. In Fig. 3, a plot similar to that in Fig. 2 is shown for the decay rates of NH_2 in the first excited vibrational state $\text{NH}_2[X^2B_1(0,1,0)]$.

For the reactions with NO,

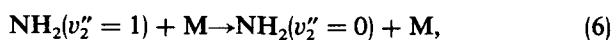


$k_{\text{NO}}(\nu_2'' = 0) = 1.4 \times 10^{-11} \text{ cm}^3 \text{ molecule}^{-1} \text{ s}^{-1}$ which is the composite decay rate constant of reactions (2a) and (3a); and $k_{\text{NO}}(\nu_2'' = 1) = 3.2 \times 10^{-11} \text{ cm}^3 \text{ molecule}^{-1} \text{ s}^{-1}$, which is the composite decay rate constant for reactions (2b) and (3b), and also includes the relaxation by NO,



The results obtained for NH_2 in $\nu_2'' = 0$ are in excellent agreement with the reported literature values, as can be seen in Table I. The values obtained for the decay rate of vibrationally excited amino radicals is more than twice that of $\text{NH}_2(\nu_2'' = 0)$. In principle, this fast decay rate (decay occurs in only a few gas kinetic collisions) can be caused not only by reaction, but also by extremely fast vibrational relaxation [Eq. (12)].

In order to observe the effect of similar collision partners on the vibrational relaxation rate of the excited vibrational state, experiments were performed using N_2 and O_2 as diatomic collision partners and Ar as an atomic collision partner.



where $\text{M} = \text{N}_2, \text{O}_2, \text{Ar}$.

The vibrational energy spacing²³ of NO, E_ν

(NO) = 1876 cm^{-1} , is between O_2 , $E_\nu(\text{O}_2) = 1556 \text{ cm}^{-1}$, and N_2 , $E_\nu(\text{N}_2) = 2331 \text{ cm}^{-1}$. Thus, the effect of O_2 and N_2 on the vibrational relaxation of $\text{NH}_2(\nu_2'' = 1)$ should be comparable to NO, especially since the vibrational energy of O_2 is comparable to ν_2'' of NH_2 [$E_\nu(\text{NH}_2) = 1498 \text{ cm}^{-1}$].^{21,23} The vibrational relaxation rate constants were $k_{\text{O}_2} = 5.3 \times 10^{-13} \text{ cm}^3 \text{ molecule}^{-1} \text{ s}^{-1}$, $k_{\text{N}_2} = 2.9 \times 10^{-13} \text{ cm}^3 \text{ molecule}^{-1} \text{ s}^{-1}$, and $k_{\text{Ar}} = 1.15 \times 10^{-13} \text{ cm}^3 \text{ molecule}^{-1} \text{ s}^{-1}$.²⁴ These results show that the vibrational relaxation (which also shows a pseudo-first-order behavior) is more than one order of magnitude less efficient than the chemical reactions, even for the most efficient collision partner. Assuming the decay rate constants to be indicative of vibrational relaxation in each case, the observed trend is as expected being highest for O_2 and lowest for Ar. Both N_2 and O_2 are expected to be more efficient than Ar in relaxing vibrational excitation since they have both rotational and vibrational degrees of freedom. We would also expect O_2 to be more efficient than N_2 as a relaxation partner, since it is only off-resonant with $\text{NH}_2(\nu_2'' = 1)$ by $\sim 58 \text{ cm}^{-1}$, whereas N_2 is off-resonant by $\sim 833 \text{ cm}^{-1}$.

If the major contribution to the observed fast decay rate for $\text{NH}_2(\nu_2'' = 1)$ in the presence of NO is due to chemical reaction, it offers an interesting contrast to the observed thermal behavior of NH_2 radicals. In the thermal studies performed by Lesclaux *et al.*⁸ and later by Silver and Kolb,⁵ a negative temperature coefficient was consistently obtained for all the observed reaction channels.

These observations suggest the existence of a long-lived intermediate complex of the type NH_2NO . The formation of such a complex is usually an exothermic process



due to the fact that a bond is formed. The rate of formation of this complex, which is a determining step in the total reaction will certainly have a negative temperature coefficient and will dominate the overall temperature behavior of the reaction. The existence of this NH_2NO complex was detected by Gehring *et al.*⁴ with the use of a mass spectrometer. Those studies were performed using NH_3 as a precursor for the amino radical. The total pressure was 2.4 Torr at room temperature, conditions which can be compared to the reactant pressure range of 50 mTorr to 3.00 Torr that was used in the present set of experiments.

Strictly speaking, the competition between reaction and

relaxation is controlled by the details of the potential energy surface. However, it has been observed that an increase in the NH_2 vibrational energy by 17.9 kJ mol^{-1} ($\nu_2'' = 1$) increases the decay rate with NO by more than a factor of 2. If the same amount of energy were to be supplied to the system through thermal heating of the amino radicals, then more than 90% of the energy would excite the translational and rotational modes of the NH_2 molecule and the temperature would increase to $\sim 800 \text{ K}$. Using the expression derived by Silver and Kolb⁵ to calculate the thermal rate of reaction for $T = 298 \text{ K}$ and $T = 800 \text{ K}$,

$$k(\text{cm}^3 \text{ molecule}^{-1} \text{ s}^{-1}) = (4.38 \times 10^{-5})T^{-2.3} \times \exp(-1360 \text{ cal mol}^{-1}/RT), \quad (14)$$

it is found that the reaction rate *decreases* by a factor of 2. Thus, channeling the energy into translational and rotational excitation of NH_2 *reduces* the reactivity. On the other hand, selective excitation of the bending vibrational mode of NH_2 results in a much more efficient decay of the vibrationally excited radical.

In other experiments²⁵⁻²⁷ involving the reaction



the reaction rate is enhanced by vibrational excitation of the bond to be broken. An increase in the vibrational energy of H_2 by 52.7 kJ mol^{-1} increased the reaction rate by a factor of 155,²⁵ while vibrational excitation of OH by 85.4 kJ mol^{-1} enhances the reactivity only by 50%.^{26,27} It would be interesting to see how the reaction rate for $\text{NH}_2 + \text{NO}$ would change when the energy is channeled into vibrational excitation of the NO molecule.

$\text{NH}_2(\nu_2'' = 1)$ decay through collisions with precursor molecules

The removal of $\text{NH}_2(\nu'' = 1)$ radicals in collisions with precursor molecules were studied both for the case of N_2H_4 and for CH_3NH_2 . The rate can be obtained, in Fig. 3, from the intercept which is the extrapolation to zero NO pressure. The influence of reaction with the precursor molecule and of vibrational relaxation can be of importance to the observed decay rate of the NH_2 radical, particularly at higher precursor pressures. The pseudo-first-order decay rate obtained for the removal of $\text{NH}_2(\nu_2'' = 1)$ by N_2H_4 is $k = 9 \times 10^{-11} \text{ cm}^3 \text{ molecule}^{-1} \text{ s}^{-1}$ and for the removal of $\text{NH}_2(\nu_2'' = 1)$ by CH_3NH_2 is $k = 7.7 \times 10^{-11} \text{ cm}^3 \text{ molecule}^{-1} \text{ s}^{-1}$. Since the contribution to the total decay of $\text{NH}_2(\nu_2'' = 1)$ from diffusion and relaxation by Ar have been shown to be quantitatively smaller than these observed decay rates, these values are a composite of reaction and vibrational relaxation via Eq. (6), where $\text{M} = \text{N}_2\text{H}_4$ and CH_3NH_2 , respectively. These values are shown in Table I and are more than a factor of 2 higher than the rates obtained for the reaction with NO.

The decay rate is slightly higher for collisions with hydrazine than for collisions with monomethylamine, but the difference is not considerable. These results indicate that collisions with precursor molecules are an important decay channel of vibrationally excited NH_2 molecules, even more than recombination processes (see the following section),

which are second-order reaction paths.

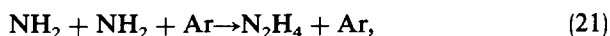
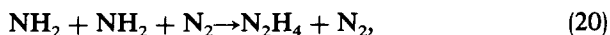
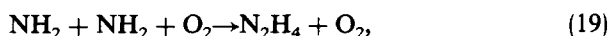
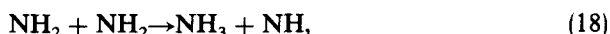
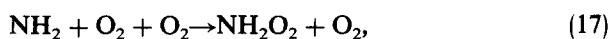
The reaction



has been reported in the literature¹⁵ as having a rate coefficient of $k = 5.3 \times 10^{-13} \text{ cm}^3 \text{ molecule}^{-1} \text{ s}^{-1}$ at 298 K , and predicts a much slower decay rate than the one observed at the pressure of 50 mTorr of N_2H_4 used in these experiments. Thus, reaction (16) can be ruled out as a significant contributor to the decay of NH_2 with the N_2H_4 precursor.

$\text{NH}_2(\nu_2'' = 0)$: Recombination reactions

The contribution of recombination radical-radical reactions can also be of importance in the observed disappearance rate of the NH_2 radical. The highly efficient and non-competitive production of NH_2 radicals from the IRMPD of N_2H_4 , offers the opportunity to study the recombination reactions of the amino radicals. The recombination reactions for $\text{NH}_2(\nu_2'' = 0)$ to be considered, excepting Eq. (17), are the following,



where N_2 , O_2 , or Ar are added as third-body collision partners.

In the case of using O_2 as a third-body collision partner, there is also the possibility of a competitive reaction according to Eq. (17) above. However, according to the results reported by Hack, Horle, and Wagner,²⁸ the rate constant expression derived for the NH_2 reaction with O_2 [Eq. (17)] leads to decay rates much lower than the experimental rates observed in this study. Even for the highest pressure of 115 Torr O_2 used in our experiments, the measured decay rate of NH_2 was much faster than the calculated rate $k_{\text{O}_2} = 4.9 \times 10^4 \text{ s}^{-1}$. This indicates that reaction (17) is, if at all, of minor importance in this study. Another strong piece of evidence which indicates that reaction (17) or a possible bimolecular process has a negligible effect on the studied NH_2 decay rate is the observed reaction order. According to reaction (17), a pseudo-first-order decay would be expected for the NH_2 temporal behavior. However, an inverse power rate law was observed, which indicates a second-order reaction, as expected from reaction channels (18)–(21).

Thus, the recombination reactions appear to be limited to reactivity according to process (18) and reformation of N_2H_4 according to processes (19)–(21).

The corresponding differential equation which describes the temporal decay of NH_2 is

$$\frac{d[\text{NH}_2]}{dt} = -k_{\text{M}}[\text{M}][\text{NH}_2]^2 - k_{18}[\text{NH}_2]^2, \quad (22)$$

where k_{M} is the rate constant characterizing reactions (19)–(21). Therefore,

$$[\text{NH}_2](t) = \frac{[\text{NH}_2]_0}{1 + [\text{NH}_2]_0(k_{\text{M}}[\text{M}] + k_{18})t}, \quad (23)$$

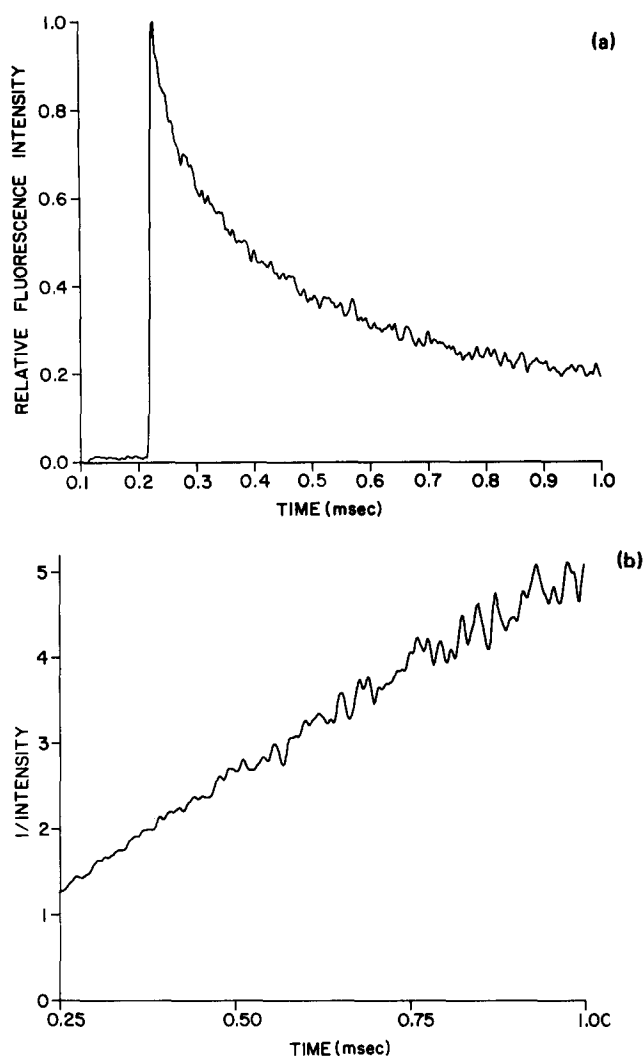


FIG. 4. Decay curve of $\text{NH}_2(\nu'' = 0)$. (a) Laser-induced fluorescence signal $\text{Int}(t)$ from $\text{NH}_2(\nu'' = 0)$ as a function of time for the second-order reactions $\text{NH}_2 + \text{NH}_2 \rightarrow \text{NH} + \text{NH}_3(1)$, and $\text{NH}_2 + \text{NH}_2 + \text{M} \rightarrow \text{N}_2\text{H}_4 + \text{M}(2)$. Pressure of gases in the system: 50 mTorr N_2H_4 and 40 Torr O_2 . (b) Plot of the inverse signal $1/\text{Int}(t)$ from (a) as a function of time. The second order rate constant $k' = [\text{NH}_2]_0(k_2[\text{M}] + k_1)$ can be obtained from the ratio of slope to intercept of the curve.

where $[\text{NH}_2]_0 = [\text{NH}_2](t = 0)$ is the initial concentration of the amino radical.

The fluorescence intensity (Int) is proportional to the NH_2 radical concentration in each single experimental run, thus $\text{Int} = [\text{NH}_2]/c$ (where c is a constant). It follows that

$$\text{Int}^{-1} = c[\text{NH}_2]_0^{-1} + c(k_M[\text{M}] + k_{18})t \quad (24)$$

so that a plot of inverse signal intensity vs time should give a

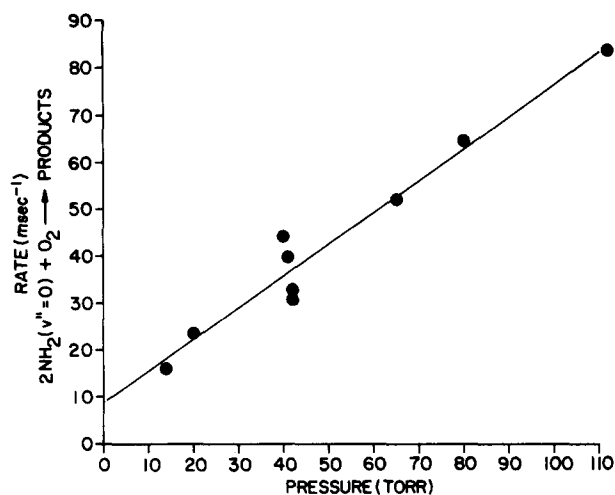


FIG. 5. Plot of the determined rate constant k' as a function of $[\text{M}]$ for $\text{M} = \text{O}_2$. From this curve, the importance of the different reaction channels $\text{NH}_2 + \text{NH}_2 \rightarrow \text{NH} + \text{NH}_3(1)$, and $\text{NH}_2 + \text{NH}_2 + \text{M} \rightarrow \text{N}_2\text{H}_4 + \text{M}(2)$ can be determined by the ratio of the intercept to slope (see the text).

straight line with slope $s = c(k_M[\text{M}] + k_{18})$ and intercept $i = c[\text{NH}_2]_0^{-1}$ [see Figs. 4(a), 4(b)]. As can be seen from Eq. (24), the ratio of the slope to the intercept gives the same expression for the decay rate constant k' as in Eq. (23):

$$k' = [\text{NH}_2]_0(k_M[\text{M}] + k_{18}). \quad (25)$$

The individual rate constants can be obtained from plots of the rate constant k' vs the third-body collision partner concentration $[\text{M}]$, so that

$$k_M = s'/[\text{NH}_2]_0, \quad (26)$$

$$k_{18} = i'/[\text{NH}_2]_0, \quad (27)$$

where s' and i' are the slope and the intercept, respectively, corresponding to Eq. (25). For the case in which O_2 was used as a third-body collision partner (Fig. 5) the following results were obtained:

$$s' = (680 \pm 60)\text{s}^{-1} \text{ Torr}^{-1} \\ \approx 2.1 \times 10^{-14} \text{ cm}^3 \text{ molecule}^{-1} \text{ s}^{-1}, \quad (28)$$

$$i' = (8.8 \pm 3.4) \times 10^3 \text{ s}^{-1}. \quad (29)$$

In order to determine the absolute values of the constants k_M and k_{18} , it would be necessary to know the initial concentration of NH_2 radicals in each experiment. However, even without knowing $[\text{NH}_2]_0$, a great deal of information can be extracted, and the importance of both reaction channels as a function of the third-body collision partner M can be determined (Table II). The ratio of k_M to k_{18} with

TABLE II. Ratios of rate constants of NH_2 recombination processes.

Reaction	$k_1/k_2(T = 298 \text{ K})$ (molecule cm^{-3})	Method	Reference
$\text{NH}_2 + \text{NH}_2 + \text{M}$	1.3×10^{17}	Flow reactor	4
$\text{NH}_2 + \text{NH}_2 + \text{O}_2$	$(4.2 \pm 1.3) \times 10^{17}$	MPD/LIF	This work
$\text{NH}_2 + \text{NH}_2 + \text{N}_2$	$(4.9 \pm 2.1) \times 10^{17}$	MPD/LIF	This work
$\text{NH}_2 + \text{NH}_2 + \text{M}$	$(1.0 \pm 0.4) \times 10^{18}$	MPD/LIF	This work

oxygen as the third-body collision partner is:

$$k_{18}/k_M (M = \text{O}_2) = (13 \pm 4) \text{ Torr} \\ = (4.2 \pm 1.3) \times 10^{17} \text{ molecule cm}^{-3}. \quad (30)$$

For 1 Torr of O_2 , 93% of the reaction would proceed through channel 18, while only 7% would react through the three-body collision path (19).

From the studies made using N_2 and Ar as third-body collision partners, Eqs. (20) and (21), the following ratios were obtained:

$$k_{\text{N}_2}/k_{\text{O}_2} = (0.85 \pm 0.25), \quad (31)$$

$$k_{\text{Ar}}/k_{\text{O}_2} = (0.04 \pm 0.01). \quad (32)$$

Equation (31) indicates that N_2 is almost as efficient as O_2 as a third-body collision partner. Ar, on the other hand, is more than one order of magnitude less efficient, which is in accordance with its larger mass, smaller size, and fewer degrees of freedom in comparison to N_2 and O_2 .

CONCLUSION

The decay of vibrationally excited amino radicals through collisions with $\text{NO}(v'' = 0)$ has been studied. The removal depends strongly on whether the NH_2 radicals are translationally, rotationally, or vibrationally excited. Excitation of the ν_2 bending vibration of NH_2 significantly enhances the decay rate, while the same amount of energy, transferred to the translation and rotation of NH_2 results in a decrease of reactivity relative to the reaction rate of 298 K.

Elementary rate constants for reactions with NH_2 in $v_2'' = 0, 1$ were obtained, as well as decay rates for $\text{NH}_2(v_2'' = 1)$ in collision with hydrazine and monomethylamine (Table I). Three different collision partners ($M = \text{O}_2, \text{N}_2, \text{Ar}$) for radical-radical recombination reactions of the kind $2 \text{NH}_2 \rightarrow \text{NH}_3 + \text{NH}(1)$ and $2 \text{NH}_2 + M \rightarrow \text{N}_2\text{H}_4 + M(2)$ were studied, and the ratio of reactions (1) to (2) is: $k(1)/k(2) = 4.2 \times 10^{17} \text{ molecule cm}^{-3}$ for $M = \text{O}_2$, $k(M = \text{N}_2)/k(M = \text{O}_2) = 0.85 \pm 0.25$ and $k(M = \text{Ar})/k(M = \text{O}_2) = 0.04 \pm 0.01$.

ACKNOWLEDGMENTS

We gratefully acknowledge support of this work by the Department of Energy through Contract No. DE-AC02-78ER04695 Mod. 005 and the National Science Foundation

through Grant No. CHE-8023362 for the equipment used in this study. Karl-Heinz Gericke would like to gratefully acknowledge the Alexander von Humboldt Foundation for its support.

- ¹J. A. Logan, M. J. Prather, S. C. Wofsy, and M. B. McElroy, *J. Geophys. Res.* **86**, 7210 (1981).
- ²A. G. Gayton and H. G. Wolfhard, *Flames*, 4th ed. (Chapman and Hall, London, 1979).
- ³W. C. Gardiner, Jr. and D. B. Olson, *Annu. Rev. Phys. Chem.* **31**, 377 (1980).
- ⁴M. Gehring, K. Hoyerman, H. Schacke, and J. Wolfrum, *Symp. Int. Combust. Proc.* **14**, 99 (1972).
- ⁵J. A. Silver and C. E. Kolb, *J. Phys. Chem.* **86**, 3240 (1982).
- ⁶G. Hancock, W. Lange, M. Lenzi, and K. H. Welge, *Chem. Phys. Lett.* **33**, 168 (1975).
- ⁷W. Hack, H. Schacke, M. Schröter, and H. Gg. Wagner, *Symp. Int. Combust. Proc.* **17**, 505 (1979).
- ⁸R. Lesclaux, P. V. Khê, P. Dezaudier, and J. C. Soulignac, *Chem. Phys. Lett.* **35**, 493 (1975).
- ⁹M. L. Lesiecki, K. W. Hicks, H. Orenstein, and W. A. Guillory, *Chem. Phys. Lett.* **71**, 72 (1980).
- ¹⁰S. E. Bialkowski and W. A. Guillory, *J. Phys. Chem.* **86**, 2007 (1982).
- ¹¹H. W. Galbraith and J. Ackerholt, in *Laser Induced Chemical Processes*, edited by J. I. Stenfeld (Plenum, New York, 1981).
- ¹²P. A. Schulz, Aa. S. Sudbo, D. J. Krajnovich, H. S. Kwok, Y. R. Shen, and Y. T. Lee, *Annu. Rev. Phys. Chem.* **30**, 379 (1979).
- ¹³D. L. Baulch, B. D. Drysdale, D. G. Horne, and A. C. Lloyd, *Evaluated Kinetic Data for High Temperature Reactions, VII* (Butterworths, London, 1973).
- ¹⁴J. D. Salzman and E. J. Bair, *J. Chem. Phys.* **41**, 3654 (1964).
- ¹⁵M. Gehring, K. Hoyerman, H. and J. Wolfrum, *Ber. Bunsenges. Phys. Chem.* **15**, 1287 (1971).
- ¹⁶S. V. Filseth, J. Danon, D. Feldmann, J. D. Campbell, and K. H. Welge, *Chem. Phys. Lett.* **63**, 615 (1979); K.-H. Gericke and W. A. Guillory (to be published).
- ¹⁷I. Messing, C. M. Sadowski, and S. V. Filseth, *Chem. Phys. Lett.* **66**, 95 (1979).
- ¹⁸A. P. Gray and R. C. Lord, *J. Chem. Phys.* **26**, 690 (1957).
- ¹⁹P. L. Giguere and I. D. Liv, *J. Chem. Phys.* **20**, 136 (1952).
- ²⁰K. Oressler and D. A. Ramsay, *Philos. Trans. A* **251**, 559 (1959).
- ²¹M. Kroll, *J. Chem. Phys.* **63**, 319 (1975).
- ²²S. E. Bialkowski, D. S. King, and J. C. Stephenson, *J. Chem. Phys.* **79**, 1156 (1980).
- ²³G. Herzberg, *Molecular Spectra and Molecular Structure, Vols. I-III*, 2nd ed. (Van Nostrand Reinhold, New York, 1950).
- ²⁴K.-H. Gericke, L. M. Torres, and W. A. Guillory (to be published).
- ²⁵R. Zellner, *J. Phys. Chem.* **83**, 18 (1979).
- ²⁶J. E. Spencer, J. Endo, and G. P. Glass, 16th Int. Symp. Combust. **16**, 829 (1977).
- ²⁷G. C. Light and J. H. Matsumoto, *Chem. Phys. Lett.* **58**, 578 (1978).
- ²⁸W. Hack, O. Horle, and H. Gg. Wagner, *J. Phys. Chem.* **86**, 765 (1982).